Supporting Information

Purohit and Auerbach 10.1073/pnas.0809272106

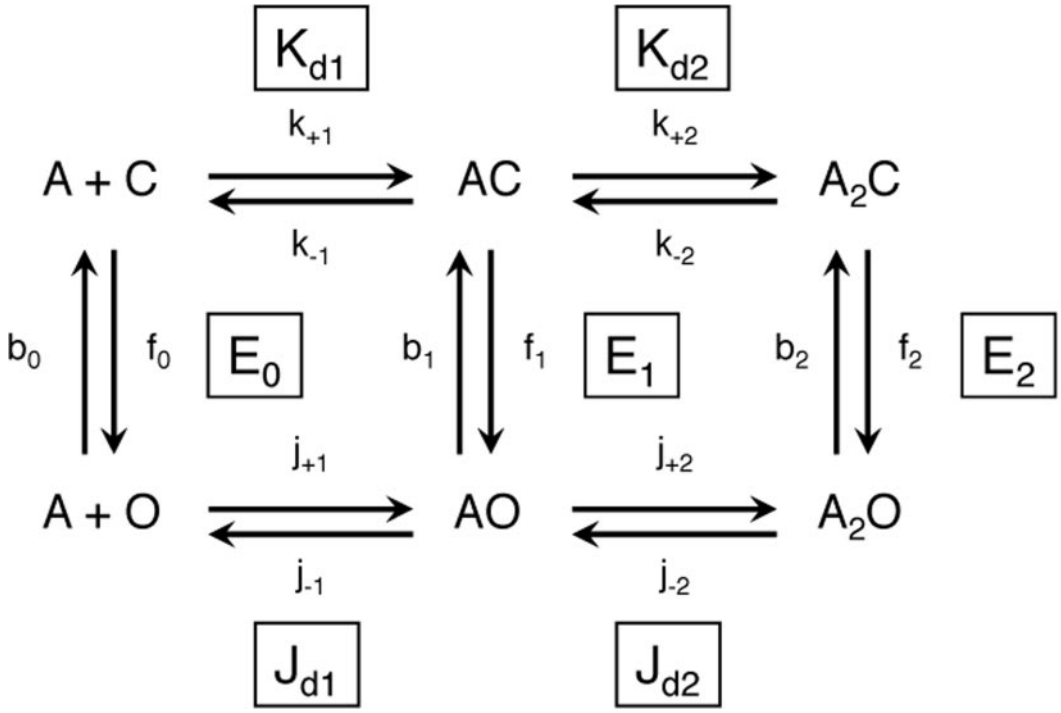

Fig. S1. State model for binding and gating. **C** is the stable, closed conformation (low-affinity for agonists and a nonconducting channel), and **O** is the stable open conformation (high-affinity and conducting). The arrows are the short-lived intermediates states that link the stable states. A is the agonist. k_+ and j_+ are the ligand association, and k_- and j_- are the ligand dissociation, rate constants in **C** vs. **O**. K_d and J_d are the corresponding equilibrium dissociation constants. f and b are the channel opening and closing rate constants; subscript is the number of bound ligands. E_0, E_1, and E_2 are the corresponding gating equilibrium constants ($= f/b$). Estimates for all parameters are shown in Fig. 5.

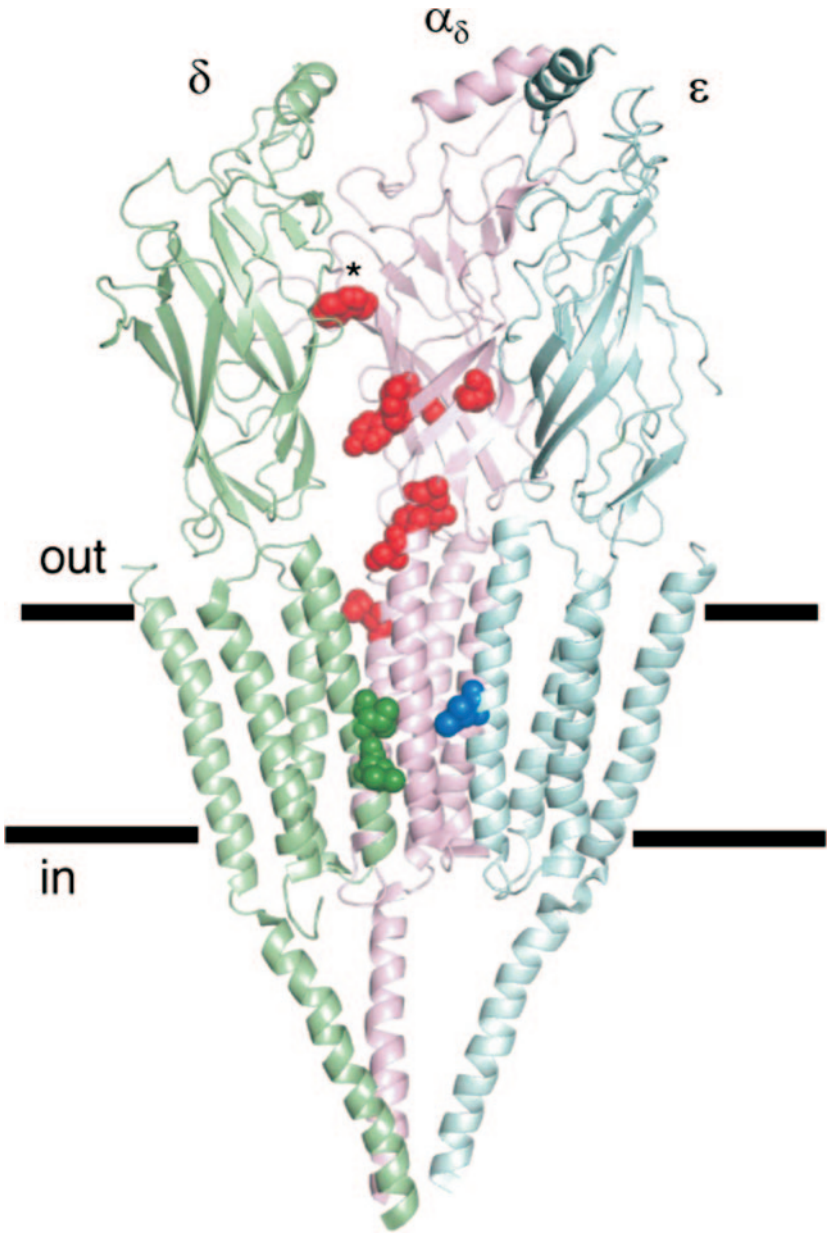

Fig. S2. Location of mutations. The $\alpha\varepsilon$ and β subunits have been removed, for clarity. The thick horizontal lines approximately mark the membrane. Subunits: α_δ, pink; δ, green; ε, blue. The mutated residues are shown as spheres (Table S1). αW149 (asterisk) marks the transmitter binding site. The other mutated α subunit residues are (*Top* to *Bottom*, approximately): D97 (loop A), Y127 ($\beta6'$ strand), M144 ($\beta7$ strand), E45 (loop 2), S52 ($\beta2$ strand), P272 (M2–M3 linker), S269 (M2; 27′) and L279 (M3, 22′). The mutated transmembrane domain residues are: green, V269 (δM2, 13′) and L265 (δM2, 9′); blue,V265 (εM2, 13′). The structural model is 2bg9.pdb.

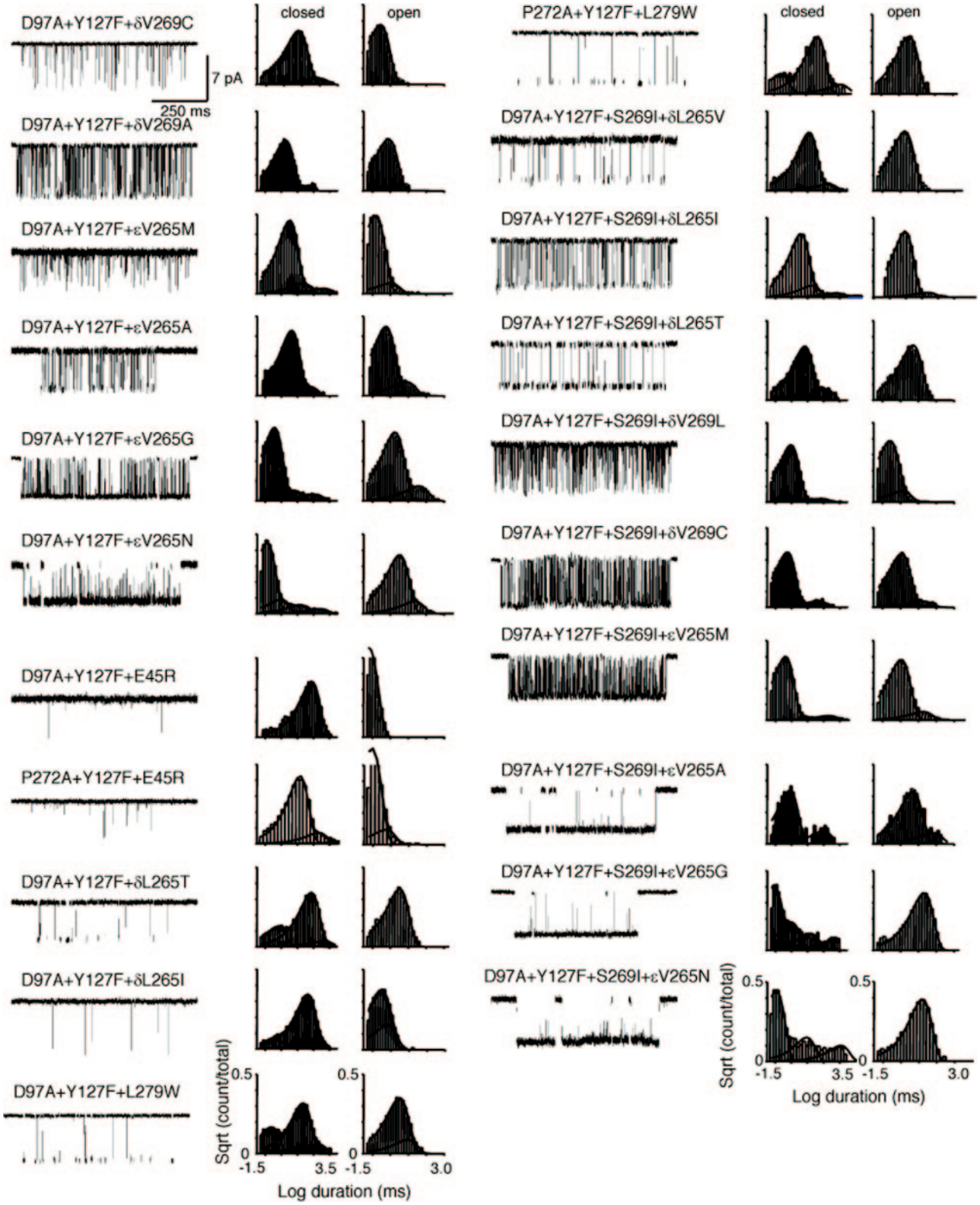

Fig. S3. Unliganded, single-channel currents and dwell-time histograms. Open is down. Unless noted otherwise, the mutations were in the α subunit. See Fig. 2 for 4 additional constructs, and Table S2.

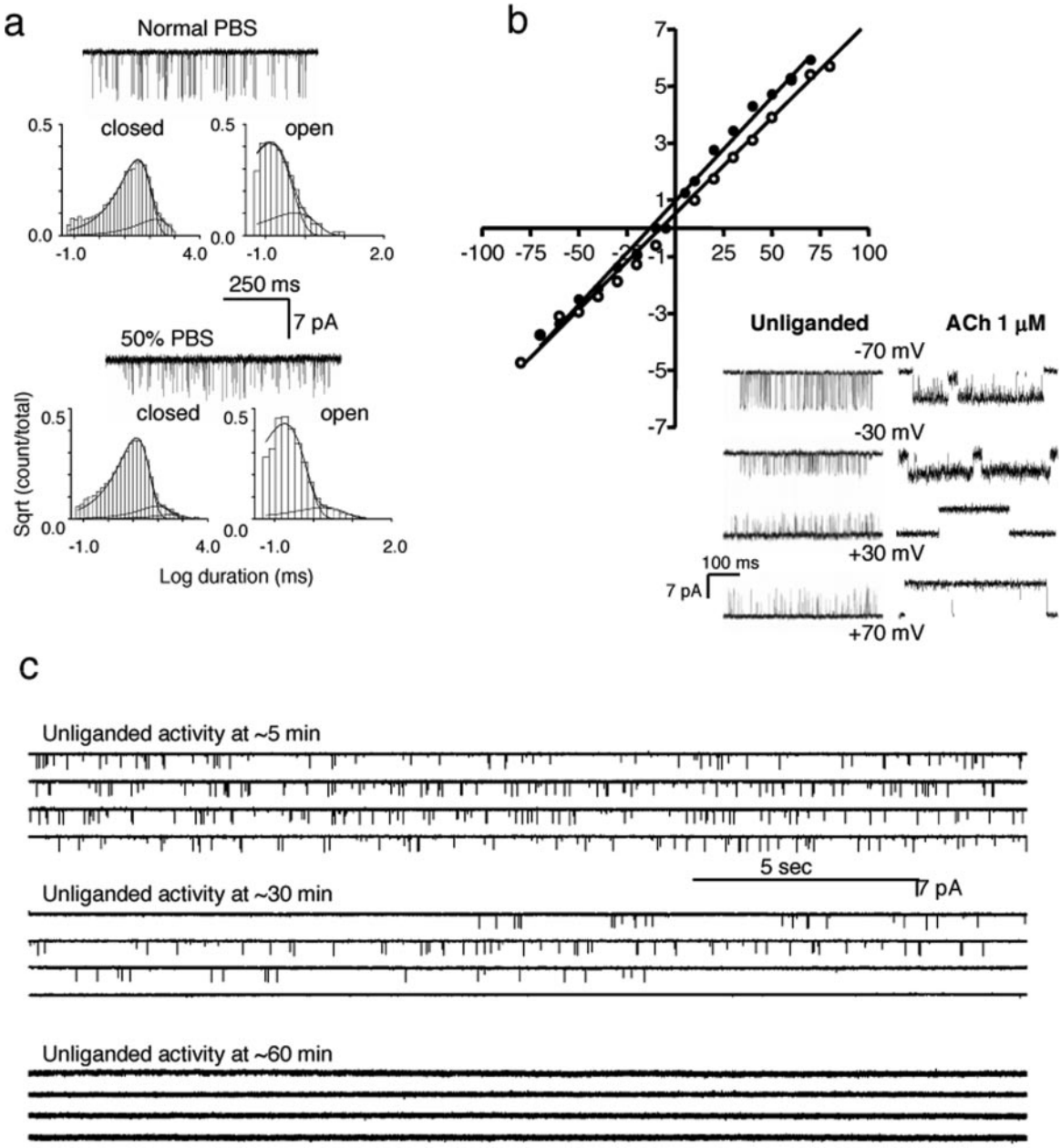

Fig. S4. Some features of unliganded gating. (*a*) Unliganded currents and interval duration histograms in different extracellular ionic strength solutions; α(D97A+Y127F+S269I). The gating rate constants are similar in both solutions (Table S2). The current amplitude was 7 pA in normal PBS and 3.5 pA in 50% PBS. (*b*) I–V relationship for unliganded single-channel openings (αD97A+αY127F+δV269T). The slope conductance is ≈67 pS, comparable with that for diliganded AChRs (72 pS). (*c*) α-Bungarotoxin blocks unliganded gating α(Y127F+P272A). The cell-attached pipette was backfilled with 100 nM toxin, which diffused the tip to gradually inhibit spontaneous openings.

Table S1. Location and effect of mutations on E_2 in AChRs

Mutant	Location		Fold-change in E_2	Ref.
	Subunit	Secondary structure		
D97A	α	Loop A	168	(1)
Y127F	α	β6′ strand	59	(2)
E45R	α	Loop 2	16.5	(3)
αS269I	α	M2–M3 linker	115	(4)
P272A	α	M2–M3 linker	218	(5)
L279W	α	M3	156	(6)
S52F	α	β2 strand	3	Unpublished data
M144L	α	β7 strand	6.5	(7)
L265V	δ	M2	0.89	(8)
L265I	δ	M2	5	(8)
L265T	δ	M2	9	(8)
V269L	δ	M2	14	(8)
V269C	δ	M2	69	(8)
V269A	δ	M2	250	(8)
V269T	δ	M2	295	(8)
V265M	ε	M2	30	Jha *et al*., unpublished data
V265A	ε	M2	245	Jha *et al*., unpublished data
V265G	ε	M2	3,098	Jha et al., unpublished data
V265N	ε	M2	15,520	Jha et al., unpublished data

The fold-change in E_2 is from experimental rate constant measurements $[[(f_2/b_2)^{mut}/(f_2/b_2)^{WT}]]$. See Fig. S2 for location in the unliganded-closed *Torpedo* AChR. Loop A is part of the TBS; αD97A does not alter K_d (1).

1. Chakrapani S, Bailey TD, Auerbach A (2003) The role of loop 5 in acetylcholine receptor channel gating. *J Gen Physiol* 122:521–539.
2. Purohit P, Auerbach A (2007) Acetylcholine receptor gating: Movement in the α subunit extracellular domain. *J Gen Physiol* 130:569–579.
3. Purohit P, Auerbach A (2007) Acetylcholine receptor gating at extracellular transmembrane domain interface: The ″Pre-M1″ linker. *J Gen Physiol* 130:559–568.
4. Mitra A, Cymes GD, Auerbach A (2005) Dynamics of the acetylcholine receptor pore at the gating transition state. *Proc Natl Acad Sci USA* 102:15069–15074.
5. Jha A, Cadugan DJ, Purohit P, Auerbach A (2007) Acetylcholine receptor gating at extracellular transmembrane domain interface: The Cys-loop and M2–M3 linker. *J Gen Physiol* 130:547–558.
6. Cadugan DJ, Auerbach A (2007) Conformational dynamics of the α M3 transmembrane helix during acetylcholine receptor channel gating. *Biophys J* 93:859–865.
7. Chakrapani S, Bailey TD, Auerbach A (2004) Gating dynamics of the acetylcholine receptor extracellular domain. *J Gen Physiol* 123:341–356.
8. Cymes GD, Grosman C, Auerbach A (2002) Structure of the transition state of gating in the acetylcholinereceptor channel pore: A Φ value analysis. *Biochemistry* 41:5548–5555.

Table S2. Effects of mutation combinations on E_0

Construct	E_2 fold-increase	f_0, s^{-1}	b_0, s^{-1}	$E_0^{construct}$	E_0^{WT}	n
D97A + Y127F + S52F	2.9×10^4	45 ± 7	6,290 ± 1,464	0.007 ± 0.001	2.4×10^{-7}	5
D97A + Y127F + S269I	1.1×10^6	187 ± 48	3,994 ± 1,106	0.048 ± 0.008	4.2×10^{-8}	8
D97A + Y127F + S269I*	—	144 ± 30	5,898 ± 774	0.025 ± 0.008	—	2
D97A + Y127F + P272A	2.2×10^6	838 ± 243	3,288 ± 89	0.25 ± 0.08	1.2×10^{-7}	3
D97A + Y127F + P272A + M144L	1.4×107	3,100 ± 91	2,457 ± 914	1.36 ± 0.54	9.7×10^{-8}	2
D97A + Y127F + S269I + εV265M	3.4×10^7	2,765 ± 635	1,804 ± 661	1.77 ± 0.85	5.2×10^{-8}	4
D97A + Y127F + S269I + εV265A	2.8×10^8	1,501 ± 91	195 ± 48	8.0 ± 2.4	2.9×10^{-8}	2
D97A + Y127F + S269I + εV265G	3.5×10^9	9,921 ± 1,210	91.7 ± 9	108 ± 5.4	3.1×10^{-8}	3
D97A + Y127F + S269I + εV265N	1.7×10^{10}	16,690 ± 357	44.3 ± 7	387 ± 124	2.2×10^{-7}	3
D97A + Y127F + εV265M	2.9×10^5	483 ± 55	8,584 ± 674	0.057 ± 0.01	1.9×10^{-7}	3
D97A + Y127F + εV265A	2.4×10^6	300 ± 11	1,343 ± 221	0.23 ± 0.04	9.5×10^{-8}	3
D97A + Y127F+ εV265G	3.0×10^7	4,512 ± 870	848 ± 185	5.34 ± 0.21	1.7×10^{-7}	3
D97A + Y127F + εV265N	1.5×10^8	9,637 ± 730	656 ± 196	15.2 ± 3.4	9.9×10^{-8}	2
D97A + Y127F + S269I + δV269L	1.6×10^7	1,560 ± 5	4,467 ± 265	0.35 ± 0.02	2.2×10^{-8}	3
D97A + Y127F + S269I + δV269C	7.8×10^7	2,010 ± 318	1,255 ± 212	1.65 ± 0.5	2.1×10^{-8}	3
D97A + Y127F + δV269C	6.8×10^5	231 ± 23	4095 ± 214	0.056 ± 0.004	8.2×10^{-8}	3
D97A + Y127F + δV269A	2.4×10^6	600 ± 71	1,500 ± 37	0.4 ± 0.06	1.6×10^{-7}	2
D97A + Y127F + S269I + δL265V	1.0×10^6	84.3 ± 20	921 ± 225	0.1 ± 0.04	9.9×10^{-8}	3
D97A + Y127F + S269I + δL265I	5.6×10^6	347 ± 124	1,275 ± 54	0.27 ± 0.1	4.7×10^{-8}	3
D97A + Y127F + S269I + δL265T	1.0×10^7	188 ± 23	169 ± 78	1.28 ± 0.7	1.2×10^{-7}	2
D97A + Y127F + δL265I	4.9×10^4	31	3,488	0.0088	1.8×10^{-7}	1
D97A + Y127F δL265T	8.9×10^4	20	314	0.064	7.2×10^{-7}	1
D97A + Y127F + E45R	1.6×10^5	39 ± 1	13,650 ± 4,664	0.003 ± 0.001	1.8×10^{-8}	3
P272A + Y127F + E45R	2.1×10^5	171 ± 2	12,810 ± 1,637	0.013 ± 0.001	6.1×10^{-8}	2
D97A + Y127F + L279W	1.5×10^6	59 ± 7	300 ± 20	0.19 ± 0.01	1.2×10^{-7}	2
P272A + Y127F + L279W	2.0×10^6	25	318	0.078	3.9×10^{-8}	1

The E_2 fold-increase is the product of the fold-increases in E_2 for each mutation (whole AChR). f_0 and b_0 are the unliganded opening and closing rate constants. $E_0^{construct} = f_0/b_0$. $E_0^{WT} = E_0^{construct}/E_2$ fold-increase; n is number of patches.
*Measured in 50% PBS. See Fig S3.